Femtosecond reaction dynamics in the gas-to-liquid transition region: Observation of a three-phase density dependence

Qianli Liu, Chaozhi Wan, and Ahmed H. Zewail

Citation: The Journal of Chemical Physics **105**, 5294 (1996); doi: 10.1063/1.472371
View online: http://dx.doi.org/10.1063/1.472371
View Table of Contents: http://scitation.aip.org/content/aip/journal/jcp/105/12?ver=pdfcov
Published by the AIP Publishing

Femtosecond reaction dynamics in the gas-to-liquid transition region: Observation of a three-phase density dependence

Qianli Liu, Chaozhi Wan, and Ahmed H. Zewail
Arthur Amos Noyes Laboratory of Chemical Physics, California Institute of Technology, Pasadena, California 91125

(Received 26 June 1996; accepted 16 July 1996)

We report the observation of a striking density dependence in the coherence dynamics of an elementary reaction, solute iodine in solvent rare gases (density from 0 to 50 mol/l). With the help of MD simulations, the time scales of *slow* and *fast* solvent-force fluctuations are resolved and the underlying mechanism is revealed. © *1996 American Institute of Physics.* [S0021-9606(96)02736-5]

I. INTRODUCTION

Studies of chemical reactions on the femtosecond time scale and in the transition from the gas to the liquid offers an opportunity to examine the influence of solvent forces on the wave packet motion of the solute. It has been demonstrated that pressure is a critical experimental variable in the studies of dense media.[1] We have previously examined the pressure dependence of collision-induced predissociation and caging of solute iodine in solvent rare gases across a wide range of 0 to 4000 bar.[2] However, a more sensitive probe of solute–solvent forces is the resolution of the phase coherence of the nuclear wave packet motion at different densities.

The relevant microscopic processes include the solute wave packet motion, the solute–solvent collisions, and the vibration–rotation coupling (centrifugal force). Accordingly, the correlation times of solute–solvent collisions (τ_{coll}) and vibration–rotation couplings ($\tau_{\text{vib-rot}}$), relative to the coherence or dephasing time (T_2) and energy relaxation (T_1), determine the observed dynamical behavior. Specifically, when the correlation times are much longer than T_2, the dynamics is controlled by a *slow modulation* of the solvent bath; when they are much shorter than T_2, a *motion narrowing* occurs and the dynamics is described by a *fast modulation* of the bath (see Refs. 3–7). As a result, the dephasing dynamics will be different in the two different regimes. Conversely, probing of how coherence and energy relaxation change with the solvent density could reveal the underlying picture of the force influence on the reaction.

In this Communication, we report our first real-time studies of the coherence dynamics (T_2 and T_1 processes) of solute iodine in solvent rare gases with the density ranging from ρ=0 to 50 mol/l (0 to 30 nm^{-3}); the reduced density $\rho^* \equiv \rho\sigma^3$ is up to 0.8. The I–I motion on the dissociative B state is the one of concern here. We resolve both the vibrational wave packet motion and the coherence decay at different densities, covering the gas-phase and the liquidlike densities in the supercritical region of the dense fluid. Furthermore, we have performed detailed molecular dynamics (MD) simulations for the same reaction in order to examine the roles of different forces. From these simulations, two snapshots of the system, together with the radial distribution and force correlation functions, are shown in Fig. 1.

II. EXPERIMENT

The experimental arrangement will be detailed later.[8] Briefly, iodine was introduced into a high-pressure cell which was filled with the pure rare gas He, Ne, or Ar. The rare gas could be compressed to a pressure between 0 and 4000 bar. The femtosecond pulse beam (620 nm), generated from a colliding-pulse mode-locked dye laser and amplified by a pulsed dye amplifier, was split into two. One of the beams, which serves as the pump, excited the iodine into its

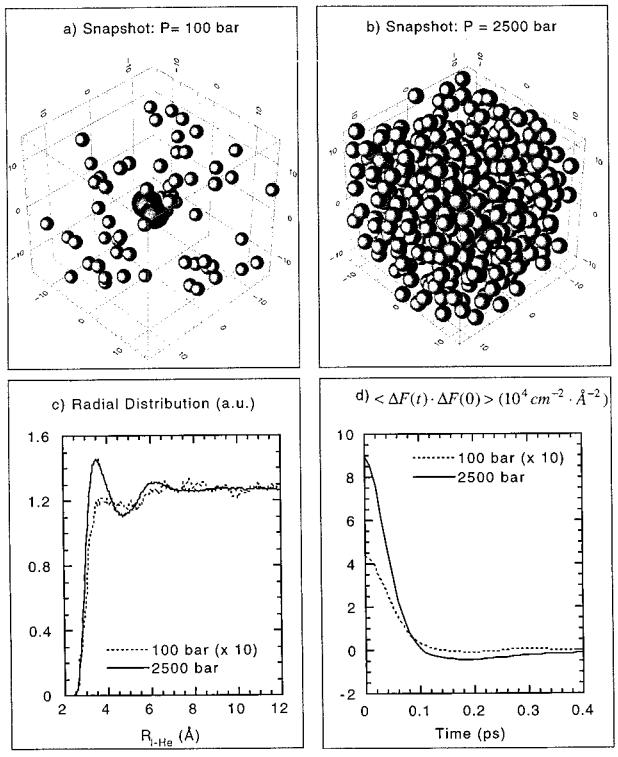

FIG. 1. MD simulations. (a) and (b): Snapshots of the iodine–helium system at 100 and 2500 bar. The two darker and larger spheres in the center represent the iodine nuclei. The smaller and lighter spheres represent the helium atoms. The sizes of iodine and helium atoms are scaled to their van der Waals diameters and the coordinates are in Å. (c) and (d): The normalized radial distribution functions (arbitrary unit), and the time correlation functions (in unit of 10^4 cm$^{-2}\cdot$Å^{-2}) of fluctuations in solute–solvent forces at the corresponding pressures. The results are averaged over more than 10^5 snapshots.

 0021-9606/96/105(12)/5294/4/$10.00

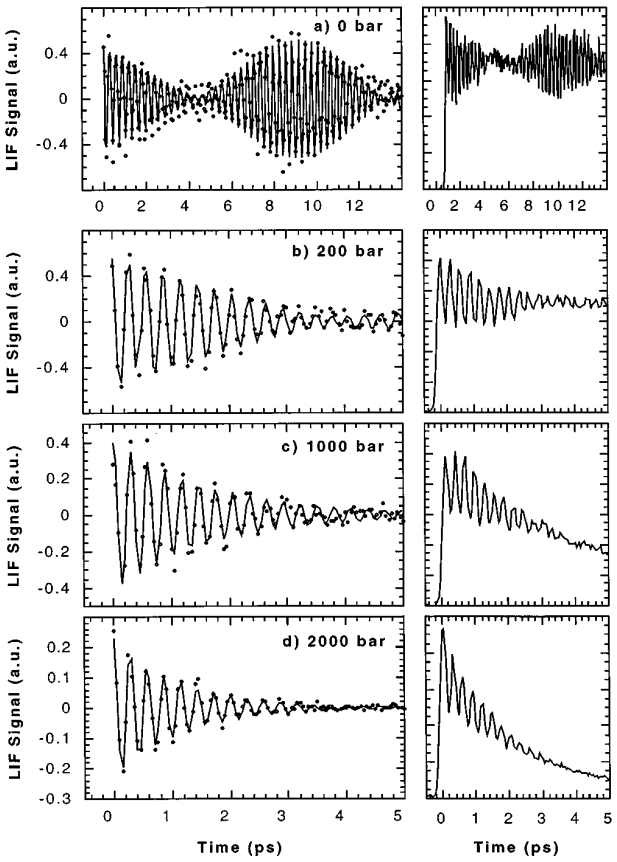

FIG. 2. Femtosecond transients for four different pressures of helium, 0 bar, 200 bar, 1000 bar, and 2000 bar (right). The transients on the left side (dots) are the corresponding results after subtraction of the decay component and the solid lines are the fit to the experimental data (see text). Similar transients were obtained for the other rare gases.

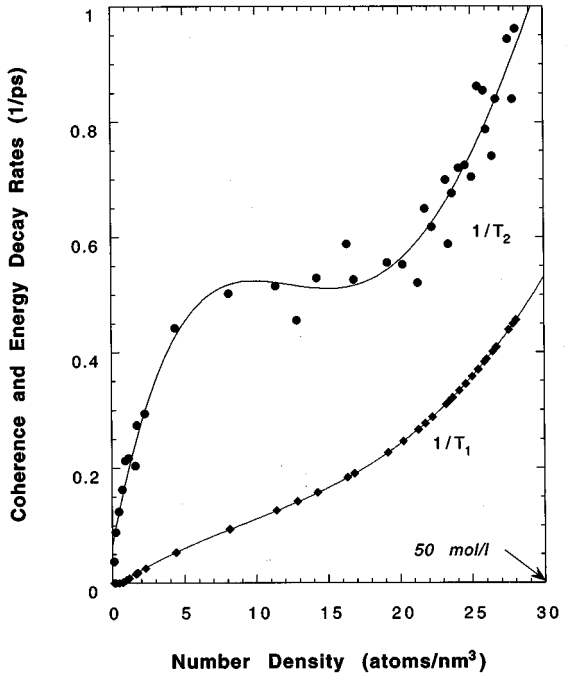

FIG. 3. The behavior of the rates ($1/T_2$ and $1/T_1$) with solvent density, here for helium (others are not shown). The lines in this figure are polynomial fit to the experimental data. The densities were obtained from the known pressure-density conversion data in Ref. 25.

B state to form a wave packet around the 8th vibration level.[9] The other beam, which was frequency-doubled to 310 nm and delayed in time by a high-precision computer-controlled actuator, was used to probe the system by laser-induced fluorescence. The pump and probe pulses were 60 fs in duration, and studies at different wavelengths were also made.[2,8] With the help of a computer, the signal was processed and recorded as a function of the relative time delay between the pump and probe pulses.

III. RESULTS AND DISCUSSION

For iodine in helium, the transients are shown in Fig. 2 for pressures ranging from 0 to 2000 bar. At 0 bar, the motion of the wave packet is observed with a period of ~300 fs. The modulation with a long time recurrence of ~10 ps is due to the anharmonicity-induced dispersion effect.[9] This long-time recurrence disappears at ~100 bar and above. At higher pressures, the average signal level also decreases with time (Fig. 2). This signal decay reflects the energy (population) relaxation of iodine on the B state (due to collision-induced predissociation, including vibrational relaxation)[8] while the decrease in the amplitude of the oscillation represents the phase spread of the wave packet. As the pressure is increased, both the energy relaxation rate ($k_1 = 1/T_1$) and the dephasing rate ($k_2 = 1/T_2$) appear to increase, but the trend for the latter is far from linear in behavior, as shown below. Similar behaviors were observed for the other rare gases.

The observed transient is best described by the following expression:[9]

$$S(t) = A + Be^{-t/T_1} + e^{-t/T_2} \sum_{i=1}^{3} C_i \cos(\omega_i t + \varphi_i), \qquad (1)$$

where A, B, and C_i's are constants, and ω_i's are the wave packet frequencies. The coherence term is obtained by subtracting the first and second terms in Eq. (1), and the experimental transients (dots) and the corresponding fits (solid lines) are plotted in Fig. 2. The behavior of the rates with density is plotted in Fig. 3. Clearly, in the raw data and in the data obtained by subtraction, the persistence of coherence over the density change studied is evident.

The striking and unexpected nonlinear behavior of $1/T_2$ with density in the gas-to-liquid transition region identifies three regimes: (i) the *low density phase* where $1/T_2$ increases rapidly with density; (ii) the *intermediate density phase* where $1/T_2$ is essentially constant, and (iii) the *high density phase* where the solvent packing is liquidlike and $1/T_2$ increases rapidly again. In simple theories of dephasing, for compressed gases one expects the rates to change linearly with density; the cross section for a T_2 process is much larger than that for T_1 (see, e.g., Refs. 6 and 10). In liquids, the repulsive or collisional process[4–6] is key to the theoretical description. Besides the repulsive force, the slowly vary-

ing attractive forces were introduced to the theory[7] to account for unusual density effects and the contributions by the different interactions. A complete description of the solvent mean force effect on the linewidth and line shift of the solute was given by separately considering the repulsive (hard sphere) and attractive contributions in a perturbed hard-sphere fluid analogy.[11] In our case, however, the reaction is experiencing different time scales of collisions (from low to high densities) and we must consider the transition for solvent modulation from the slow to the fast regime.

With MD simulations, we can address the nature of such behaviors and quantify the density at which the transition is expected. To simulate the systems under study, a given number of molecules are selected in a cubic cell and a periodic boundary condition[12] is used. With proper preparation,[8] the initial positions and velocities of the system represent the thermal distribution of such system at room temperature. Both classical and semiclassical calculations were carried out. In the former, the I_2 vibration mode was treated classically as well as the rotation and the translation modes. In the latter, the I_2 vibration mode was treated quantum mechanically while all other degrees of freedom were considered classically. The semiclassical approach adopted here shares some similarity with a recent simulation work.[13] To describe the solute–solvent and solvent–solvent interactions, we used pairwise potential models. The methodology and potential parameters will be detailed in Ref. 8.

In the classical approximation, the vibration correlation function $\langle Q(t)Q(0)\rangle$, where Q is the I–I bond stretch, was directly evaluated and its decay gave the dephasing rate $1/T_2$. The decay of the correlation function was found to be dominated by a Gaussian shape at low densities; as density was increased, the shape transformed more into an exponential form. The Gaussian and exponential shapes represent the ''slow'' and the ''fast'' modulation regimes, respectively.[3] The dephasing rates $(1/T_2)$ obtained from these classical calculations are plotted in Fig. 4. The energy relaxation time (T_1), which represents the time during which the vibrational energy of I_2 has decayed to half of the initial value, is also plotted in the same figure. In contrast to that of $1/T_2$, the density dependence of $1/T_1$ shows the usual near-linear behavior. Simulation results for Ne and Ar are similar and will be presented in Ref. 8. The classical simulations agree well with our experimental observations, suggesting their adequacy ($k_BT=200$ cm^{-1}; $\hbar\omega\sim100$ cm^{-1}). However, to reveal the underlying mechanism, we needed to examine the nature of different acting forces. This is achieved by invoking a semiclassical approach in which the vibration correlation function was related to the time integral of force correlation functions (see Refs. 5, 7, and 14).

Two types of forces are of relevance here. One is the real collision (or external[13]) force F_R which originates from the solute–solvent intermolecular interactions. The other is the rotation-induced centrifugal force, or vibration-rotation coupling.[15] In the simulation, F_R was calculated by summing over all pairwise interaction forces projected onto the I–I coordinate. Since the centrifugal force is proportional to the iodine rotational energy $E_{\rm rot}$, its behavior was studied by simulating the rotational energy change with time.

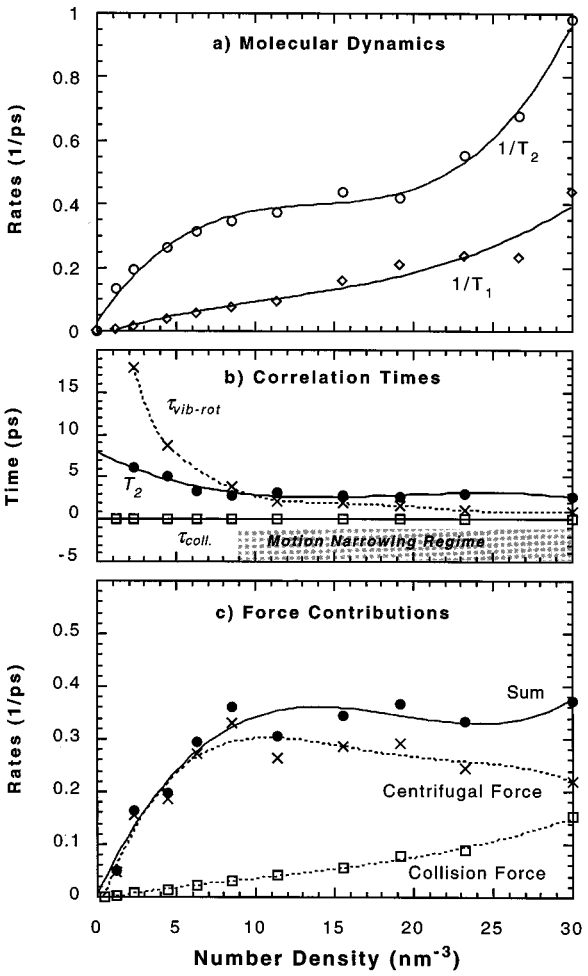

FIG. 4. MD simulation results for the helium system: (a) The classical simulation results for the energy relaxation rate $1/T_1$ (open diamond) and the dephasing rate $1/T_2$ (open circle) as described in the text. The lines are polynomial fit to the calculated results. (b) The correlation times for the vibration–rotation coupling ($\tau_{\rm vib\text{-}rot}$, cross) and the collision force ($\tau_{\rm coll}$, open square), and the dephasing time (T_2, filled circle) as functions of the solvent density. The lines are drawn smoothly through the calculated results to help guide the eyes. The shaded area indicates the region when $\tau_{\rm vib\text{-}rot}$ is shorter than T_2, the motion-narrowing regime. (c) Semiclassical results elucidating the different contributions: open squares for dephasing rates induced by the solute–solvent collision forces; cross for the vibration–rotation induced dephasing rates; and the filled circle for their sum. The lines are polynomial fit to the calculated results.

The time scales of fluctuations of the collisional and centrifugal forces are described by their correlation times $\tau_{\rm coll}$ and $\tau_{\rm vib\text{-}rot}$, respectively. They correspond to the duration of collisions and the time interval between collisions,[7,15] respectively. As shown in Fig. 4, we obtained $\tau_{\rm coll}\ll\tau_{\rm vib\text{-}rot}$ in the whole density range considered. We can, therefore, separately evaluate the correlation functions of the two forces following Schweizer and Chandler.[7] It is worth noting that we have not attempted to separate the repulsive and attractive forces. For the rare-gas systems considered, the attractive force is orders of magnitude smaller than the repulsive force; its contribution to the dephasing rate is negligible here.

Within the density range of 0 to 30 atoms/nm^3, τ_{coll} is much shorter than the dephasing time T_2 (see Fig. 4) so that the fast modulation approximation applies and the F_R induced dephasing rate $T_{2;R}^{-1}$ is proportional to $\Delta_R^2 \cdot \tau_{\text{coll}}$,[3,7] where $\Delta_R^2 \equiv \langle (\Delta F_R)^2 \rangle$ is the amplitude of the force correlation function. Since τ_{coll} is nearly constant in this regime, $T_{2;R}^{-1}$ is, therefore, proportional to Δ_R^2 which increases rapidly with the solvent density. In contrast, the dephasing rate, $T_{2;\text{vib-rot}}^{-1}$, induced by the vibration–rotation coupling behaves very differently (Fig. 4). In the motion-narrowing regime (shaded region in Fig. 4), the amplitude of the correlation function $\langle \Delta E_{\text{rot}}^2 \rangle \equiv \Delta_{\text{rot}}^2$ is nearly constant, because the rotational energy is equilibrated with the thermal bath and its change is on the order of $k_B T$. However, $\tau_{\text{vib-rot}}$ continues to decrease (see Fig. 4) and $T_{2;\text{vib-rot}}^{-1}$ therefore decreases. At low densities, $\tau_{\text{vib-rot}}$ is long compared to the dephasing time (slow modulation) and $T_{2;\text{vib-rot}}^{-1}$ is only proportional to Δ_{rot} which increases with density until reaching the limiting value of $k_B T$.

The dynamical behavior with density is now understood. At densities below 20 atoms/nm^3, $T_{2;R}^{-1}$ is much smaller than $T_{2;\text{vib-rot}}^{-1}$ (see Fig. 4). Since $T_{2;\text{vib-rot}}^{-1}$ is directly associated with the rotation of the solute, its maximum value is very nearly the same for all three solvent systems (He, Ne, and Ar) considered, as observed experimentally. At liquid densities, the collision force becomes dominant and causes the dephasing rate to increase rapidly again. The plateau is caused by the influence of the two forces which have opposing trends (Fig. 4). The significance of the vibration–rotation coupling has been found in several other systems,[13,16–20] and in the motion-narrowing regime, the dephasing by vibration–rotation coupling was predicted to be proportional to the correlation time.[7,15]

In conclusion, while the origin of T_1 process is due to collision-induced predissociation (energy exchange), the T_2 process originates from the fluctuations in the solute–solvent interactions which destroy the coherence of the reaction wave packet. At the highest density ($\rho^* \sim 1$), the collision-induced predissociation time is near 2 ps for He and 0.6 ps for Ar, consistent with the first picosecond measurement in liquids (limiting value $\sim$10 ps),[21] direct recovery measurements,[22] and recent MD simulations,[23] but much longer than the value of recent femtosecond study in liquids ($T_2 = T_1 \sim 230$ fs).[24] However, our T_2 is about 400 fs at the liquid density (Ar). The three-phase density dependence observed here reflects the different impact of the two forces, collisional and centrifugal, on the solute vibrational dynamics, with the two regimes of correlation times established. The MD reveals the underlying microscopic mechanism and elucidates the time scales of various processes critical to the dynamics of solvent-induced fluctuations.

ACKNOWLEDGMENTS

Most of the simulation works were performed on the Delta parallel supercomputer located at Caltech. The authors are grateful to Professor Vincent McKoy for providing the access to the supercomputer. We thank Mr. Chris Hyland, Dr. Cristoph Lienau, and Mr. Manish Gupta for their help in the initial phase of the work and Professor David Chandler for helpful discussions.

[1] J. Jonas, J. Chem. Soc. Faraday Tans. 2 **83**, 1777 (1987); J. Schroeder and J. Troe, Annu. Rev. Phys. Chem. **38**, 163 (1987).
[2] C. Lienau, J. C. Williamson, and A. H. Zewail, Chem. Phys. Lett. **213**, 289 (1993); C. Lienau and A. H. Zewail, *ibid.* **222**, 224 (1994).
[3] R. Kubo, in *Fluctuations, Relaxation and Resonance in Magnetic Systems*, edited by D. t. Haar (Plenum, New York, 1962).
[4] S. F. Fischer and A. Laubereau, Chem. Phys. Lett. **35**, 6 (1975).
[5] D. W. Oxtoby, Adv. Chem. Phys. **40**, 1 (1979).
[6] D. J. Diestler and J. Manz, Mol. Phys. **33**, 227 (1977); K. E. Jones, A. H. Zewail, and D. J. Diestler, in *Advances in Laser Chemistry*, edited by A. H. Zewail (Springer-Verlag, New York, 1978), p. 258; see also p. 196.
[7] K. S. Schweizer and D. Chandler, J. Chem. Phys. **76**, 2296 (1982).
[8] Q. Liu, C. Wan, and A. H. Zewail, J. Phys. Chem. (to be published).
[9] M. Gruebele and A. H. Zewail, J. Chem. Phys. **98**, 883 (1993).
[10] J. Chesnoy and J. J. Weis, J. Chem. Phys. **84**, 5378 (1986).
[11] D. Ben-Amotz and D. R. Herschbach, J. Phys. Chem. **97**, 2295 (1993).
[12] M. P. Allen and D. J. Tildesley, *Computer Simulation of Liquids* (Oxford University Press, New York, 1992).
[13] J. P. J. Michels, M. I. M. Scheerboom, and J. A. Schouten, J. Chem. Phys. **103**, 8338 (1995).
[14] W. G. Rothschild, J. Chem. Phys. **65**, 455 (1976).
[15] S. R. J. Brueck, Chem. Phys. Lett. **50**, 516 (1977).
[16] R. Kroon, R. Sprik, and A. Lagendijk, Chem. Phys. Lett. **161**, 137 (1989).
[17] R. Kroon, M. Baggen, and A. Lagendijk, J. Chem. Phys. **91**, 74 (1989).
[18] B. Lavorel, B. Oksengorn, D. Fabre, R. Saint-Loup, and H. Berger, Mol. Phys. **75**, 397 (1992).
[19] M. I. M. Scheerboom and J. A. Schouten, Phys. Rev. E **51**, R2747 (1995).
[20] A. D. May, J. C. Stryland, and G. Varghese, Can. J. Phys. **48**, 2331 (1970).
[21] T. J. Chuang, G. W. Hoffman, and K. B. Eisenthal, Chem. Phys. Lett. **25**, 201 (1974).
[22] D. E. Smith and C. B. Harris, J. Chem. Phys. **87**, 2709 (1987).
[23] M. Ben-Nun and R. D. Levine, Chem. Phys. **201**, 163 (1995).
[24] N. F. Scherer, D. M. Jonas, and G. R. Fleming, J. Chem. Phys. **99**, 153 (1993).
[25] R. D. McCarthy, J. Phys. Chem. **R.2**, 923 (1973).